

- ropylnorephedrine **4d** were obtained in a 68% yield by reductive alkylation of **4a** with acetone and sodium cyanoborohydride<sup>7</sup>: for detailed procedure and physical properties of the products **4c-f**, see experimental section.
6. Tlahuext, H.; Contreras, R. *Tetrahedron: Asymmetry* **1992**, *3*, 727.
  7. Ohfuné, Y.; Kurokawa, N.; Higuchi, N.; Saito, M.; Hashimoto, M.; Tanaka, T. *Chem. Lett.* **1984**, 441.
  8. Cho, B. T.; Chun, Y. S. *Tetrahedron: Asymmetry* **1992**, *3*, 1539.
  9. In a separate experiment, we observed that the complete reduction of acetophenone and 2-heptanone with 1 equiv of borane-THF at room temperature required for 3 h and 0.5 h, respectively.
  10. Brown, H. C.; Kramer, G. W.; Levy, A. B.; Midland, M. M. *Organic Synthesis via Boranes*; Wiley Interscience: New York, 1975; Chapter 9.
  11. Zweifel, G.; Brown, H. C. *J. Am. Chem. Soc.* **1963**, *85*, 2066.
  12. Joshi, N. N.; Srebnik, M.; Brown, H. C. *Tetrahedron Lett.* **1989**, *30*, 5551.
  13. Brown, H. C.; Choi, Y. M.; Narasimhan, S. *J. Org. Chem.* **1982**, *47*, 3153.
  14. Mckennon, M. J.; Meyers, A. I.; Drauz, K.; Schwarm, M. *J. Org. Chem.* **1993**, *58*, 3568.
  15. Itsuno, S.; Nakano, M.; Miyazaki, K.; Masuda, H.; Ito, K.; Hirao, A.; Nakahama, S. *J. Chem. Soc., Perkin Trans. 1*, **1985**, 2039.
  16. Brenner, M.; Huber, W. *Helv. Chim. Acta* **1953**, *36*, 1109.
  17. Quallich, G. J.; Woodall, T. M. *Tetrahedron Lett.* **1993**, *34*, 4145.

## Study on Equivalent Circuits of Sodalite Type Materials by Complex Impedance Analysis

Chy Hyung Kim and Kyu Seomoon

Department of Chemistry, Chongju University, Chongju 360-764, Korea

Received August 10, 1994

Electrical characteristics of Fe-substituted sodalites were analyzed and equivalent circuits of samples were designed using impedance and admittance data. Internal components of resistances ( $R_e$ ,  $R_b$ , and  $R_{gb}$ ) and capacitances ( $C_b$ ,  $C_d$  and  $C_D$ ) could be extracted by changing the frequency of measurement at three different temperatures. Upon increasing the temperature, electrical properties of the samples could be elucidated in detail by equivalent circuit. The substitution of Fe on Al site was indirectly confirmed by ESCA and the results explain the lower polarity in Na-O bond of Fe 10 mole %-substituted sodalite.

### Introduction

Isomorphous substitution of Al by Fe up to 25 mole % in sodalite framework has been carried out and its ionic semiconducting property has been studied.<sup>1</sup> For a conductivity measurement of polycrystalline materials, it is well known that AC method has many advantages because interfacial polarization between the blocking electrode-material (electrolyte) and grain boundary effects can be sorted out at proper frequencies. This method has been used by many scientists, especially for various solid electrolytes.<sup>2-9</sup>

The complex method originates from Cole and Cole complex permittivity diagrams.<sup>10</sup> The complex admittance ( $Y$ ) can be expressed as the sum of the conductance ( $G$ ) and the susceptance ( $B$ ).

$$Y = G + iB$$

Again, the complex impedance ( $Z$ ) which is reciprocal of complex admittance ( $Y^{-1}$ ) separates into real and imaginary components, *i.e.*

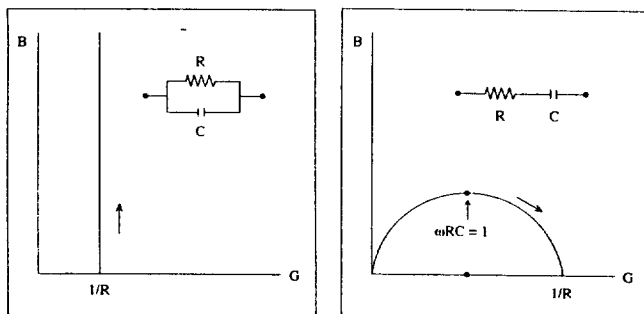
$$Z = R + jX$$

Where  $R$  is resistance and  $X$  is reactance. From the plot of  $B$  vs.  $G$  (Scheme 1), the resistance value can be derived from the circular arc intercept on the  $G$ -axis, and the capacitance value from the expression involving the frequency at the peak of the circular arc. When the admittance plot gives a circular arc, a series R-C circuit is dominant, whereas a straight line indicates more characteristic parallel R-C circuit as can be seen in Scheme 1.

Here we report new results on polycrystalline solids in extension of our previous work.<sup>1</sup> And we designed equivalent circuits of Fe-substituted sodalites by analysing the electrical data; the contribution of electronic resistance, resistances of grain and grain boundary, bulk capacitance, capacitance of electrode-material (electrolyte) interface, and dipole capacitance. These interpretations will facilitate the understanding of electrical characteristics and applications. ESCA analysis was also carried out to obtain relative compositions of samples and compare the bond polarity. Results were discussed in

**Table 1.** Conductivity and Electronic Contribution of Samples (Numbers in the parenthesis represent  $\times 10^{-4}$ )

Fe mole % $t$ ( $^{\circ}\text{C}$ )	Conductivity ( $\Omega \text{ cm}$ ) <sup>-1</sup> , Electronic Contribution (%)					
	0%	5%	10%	15%	20%	25%
205 $^{\circ}\text{C}$	4.8(-7), 96	5.5(-7), 100	9.0(-6), 10	5.5(-7), 91	5.1(-7), 100	4.5(-7), 100
325 $^{\circ}\text{C}$	2.0(-6), 23	2.2(-6), 25	1.8(-4), 2	3.4(-6), 15	3.5(-6), 15	3.5(-6), 14
450 $^{\circ}\text{C}$	1.7(-5), 4	2.8(-5), 4	1.5(-3), 1	4.2(-5), 2	5.5(-5), 2	5.3(-5), 7

**Scheme 1.** Admittance plots for simple R-C circuit.

connection with the electrical characteristics of the samples.

### Experimental

Sodalite and Fe-substituted sodalites were synthesized according to our previous report.<sup>1</sup> The pellets of the powdered samples were prepared by pressing and sintering at reaction temperatures. Blocking Au electrodes were applied to both sides of the pellets using vacuum deposition. The conductivities were measured by pulse, DC, and AC methods<sup>11</sup> at 205  $^{\circ}\text{C}$ , 325  $^{\circ}\text{C}$ , and 450  $^{\circ}\text{C}$  in a predried nitrogen atmosphere. Then the results obtained by pulse and AC method were compared to find out whether those are in good agreement.

In pulse measurement, voltage pulse of 0.8 V, pulse width 100  $\mu\text{sec}$ , and pulse duration time 500  $\mu\text{sec}$  were utilized with PG 1990 Pulse Generator of ED Engineering Company and Trio Oscilloscope CS-1040. In DC measurement, 0.5 V from a constant source was applied. Pulse method measures the instantaneous current by putting a short DC voltage pulse across a circuit containing the sample in series with a known resistor. When the circuit is closed, the instantaneous current and voltage is used to measure the total current. On the other hand, DC method measures final stabilized current which is related to the electronic conductivity, where blocking electrodes are used. Thus, from the two measurements the ionic conductivity and electronic conductivity can be sorted out, *i.e.*

$$\sigma_{\text{total}} = \sigma_{\text{ion}} + \sigma_{\text{electronic}}$$

The complex impedance and admittance were measured in frequency range 5 Hz to 13 MHz keeping 0.1 V across the sample by using Hewlett-Packard 4192 LCR meter. The experimental data were selected in the frequency range 500 Hz to 2 MHz (5 Hz to 2 MHz at 450  $^{\circ}\text{C}$ ) because the cell impedance was not negligible at high frequency and the reliability accuracy of the LCR meter was in that frequency range.

**Table 2.** ESCA Binding Energies of each elements in the Fe-substituted Sodalites (unit : eV)

Fe %	Al 2p	Si 2p	Na 1s
Zero	74.1	102.3	1072.5
5	73.9	102.2	1071.0
10	73.9	102.2	1071.0
15	73.7	102.1	1071.1
20	73.4	101.8	1071.2

ESCA spectra were recored on a VG ESCALAB MK-II spectrometer with a monochromatic Mg K $\alpha$  X-ray source. For ESCA analysis, powder samples were pressurized into pellet ( $\phi$  10 mm, thickness 2 mm) with a pressure of 1 ton/cm<sup>2</sup>. ESCA spectra were obtained after Ar<sup>+</sup> ion sputtering to remove surface contaminations for 5 minutes in a vacuum chamber. Charge compensation is accomplished by setting the binding energy of internal C 1s peak to 284 eV, which is always detected in an ESCA chamber.

### Results and Discussion

Table 1 lists the total conductivity and percentage of electronic contribution obtained by pulse and AC measurements. At 205  $^{\circ}\text{C}$ , the electronic contributions are more than 90% and the ionic portions are small, which means that thermal energy for the ionic movement is not enough below 205  $^{\circ}\text{C}$  except Fe 10 mole %-substituted sodalite.

According to the quantification data of ESCA, atomic percentage of sodium of Fe 10 mole %-substituted sodalite was lower than those of other samples although the synthetic conditions of all the samples were the same. Samples have theoretical composition of Na<sub>8</sub>Si<sub>6</sub>Al<sub>6-x</sub>Fe<sub>x</sub>O<sub>24</sub>Cl<sub>2</sub> ( $x$  : 0-1.5). Considering the magnitude of quantification error of ESCA, especially large error for the minor component, compositions of synthetic samples fit quite well with the theoretical value, except for Fe 10 mole %-substituted sodalite in which sodium was detected as 5.9 not as 8. This discrepancy in sodium composition and conductivity can be explained as follows : sodium itself is volatile at high temperature. When 10 mole % Al ions are replaced by Fe ions, Na ion shows the maximum flexibility<sup>1</sup> by weakening the bonds with the oxygen ions and neighboring sodium ion. Thus the sodium is vaporized easily and the increment of flexibility of sodium ion can induce lower activation energy for the conductivity.

ESCA binding energies of some elements are listed in Table 2. Binding energies of all metallic elements shifted to higher level than those of pure metal, so chemical states of these elements are assumed to be in the form of oxide.<sup>11</sup>

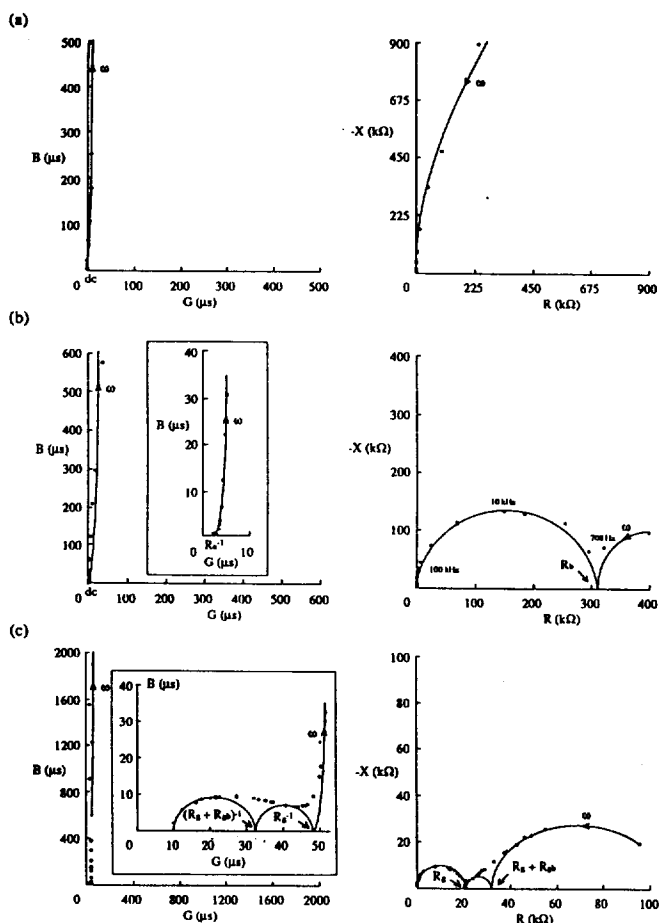


**Figure 1.** Plots of impedance and admittance for sodalite at (a) 205 °C, (b) 325 °C, and (c) 450 °C.

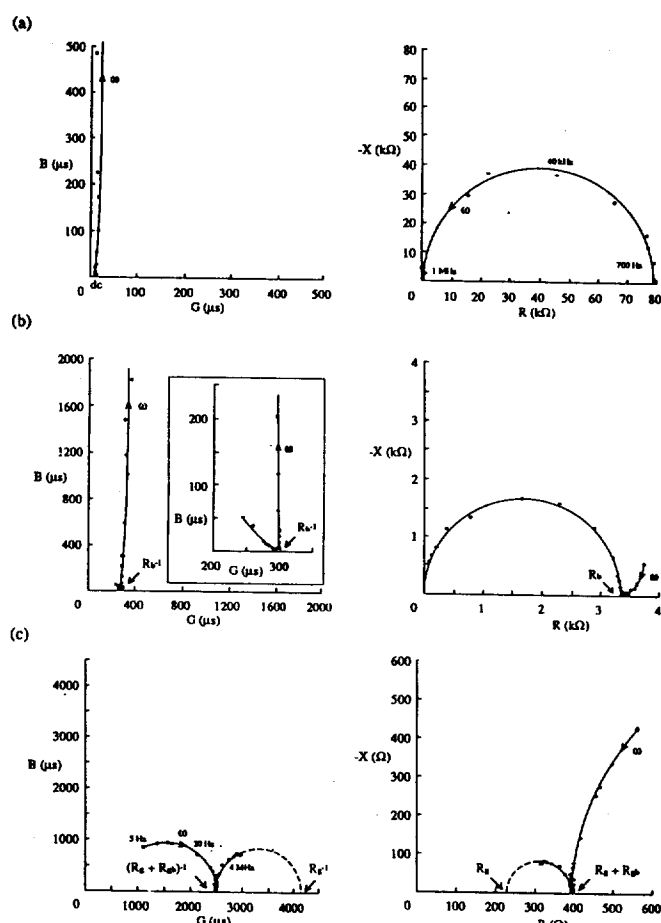


**Figure 2.** Plots of impedance and admittance for 10 mole % Fe-sodalite at (a) 205 °C, (b) 325 °C, and (c) 450 °C.

From the data of Table 2 and XRD patterns which has been reported in the previous paper,<sup>1</sup> it is reasonable that Fe atoms are substituted on the Al sites.

As the contents of substituted Fe atom increase, binding energies of Si 2*p* and Al 2*p* electron shifted gradually to the lower level, while binding energy variance of Fe 2*p* and O 1*s* was negligible. This trend can be understood in terms of bond polarity: Binding energies of O 1*s* in pure Fe<sub>2</sub>O<sub>3</sub>, Al<sub>2</sub>O<sub>3</sub>, and SiO<sub>2</sub> are known as 530, 531.6, and 533 eV respectively.<sup>12</sup> So, electron density around O atoms can be assumed in order of Fe<sub>2</sub>O<sub>3</sub> > Al<sub>2</sub>O<sub>3</sub> > SiO<sub>2</sub>, and bond polarity as Fe-O > Al-O > Si-O. Al (or Fe), Si atoms which are placed on the edge of sodalite unit cell are bonded together in the form of O-bridge, that is, Al (or Fe)-O-Si. When Fe atom is substituted on Al site, Fe atom neighbored O atom withdraws more electrons from the Fe atom, and releases some electrons to the adjacent Si or Al atom. Thus, Al-O and Si-O bonds are less polarized, and binding energies of Al and Si shift to the lower level.

Binding energies of Na atoms which are placed on the inner side of sodalite unit cell showed the minimum value at 5-10% Fe-substituted sodalite. It means that electron density around Na atom is in a maximum, and polarity of Na-O bond is in a minimum state at that condition, weakening the Na-O bond.

The plots of reactance ( $-X$ ) vs. resistance ( $R$ ) and susceptance ( $B$ ) vs. conductance ( $G$ ) of each sample at three temperatures are drawn in Figure 1-4. All the samples except Fe 10 mole %-substituted sodalite show similar patterns at 205 °C. They had electronic conductivity mainly and the magnitudes were very low ( $10^{-7} \Omega^{-1} \text{ cm}^{-1}$ ). Long range charge migration did not occur and the capacitances were almost independent on the change of frequency. Electrical double layer was not formed at the interface of blocking electrode-material so the capacitance observed at 205 °C came from the bulk (= grain + grain boundary) capacitance,  $C_b$  (about 45 pF) of the material. The equivalent circuits can be proposed as in Figure 5(a).

At 320 °C, magnitude of electronic resistance,  $R_e$  was the same as that at 250 °C, but the relative contribution was about 20% of the total conductivity. The other 80% showed ionic conductivity. This long range migration causes capacitance at the electrode-material interface which is designated as  $C_{dl}$ . Total capacitance was 1 nF at low frequency and  $C_{dl}$  component could be eliminated at above 10 kHz. Analyzing the plots, the overall behavior is dominated by the parallel arrangement of  $C_b$ , bulk resistance  $R_b$ , and  $R_e$  at high frequency with a series combination of  $C_{dl}$  at low frequency as shown in Figure 5(b). Also separations of  $R_b$  of some samples to  $R_e$  and  $R_{gb}$  were carried out using a simple method

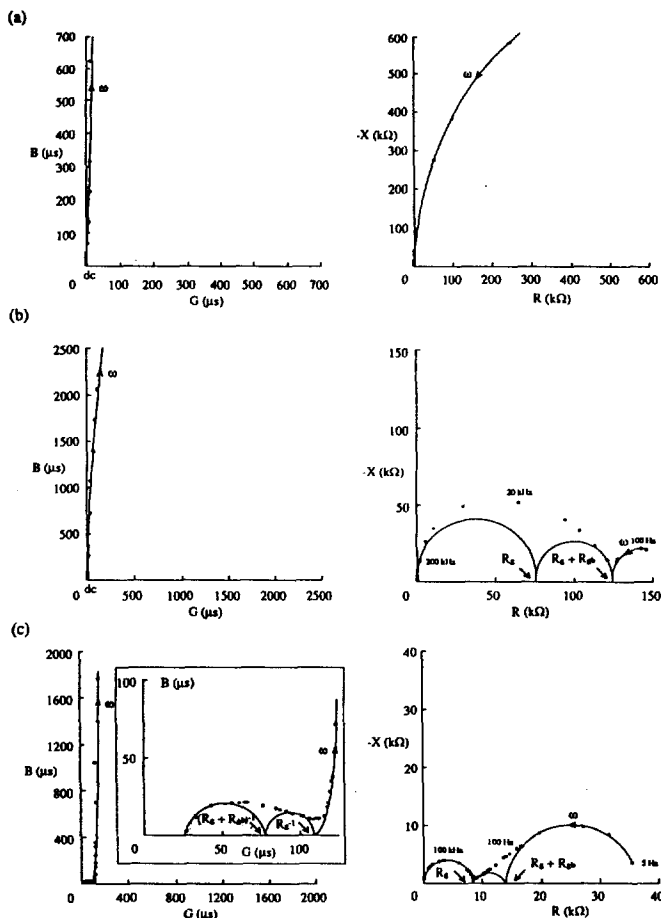


Figure 3. Plots of impedance and admittance for 15 mole % Fe-sodalite at (a) 205 °C, (b) 325 °C, and (c) 450 °C.

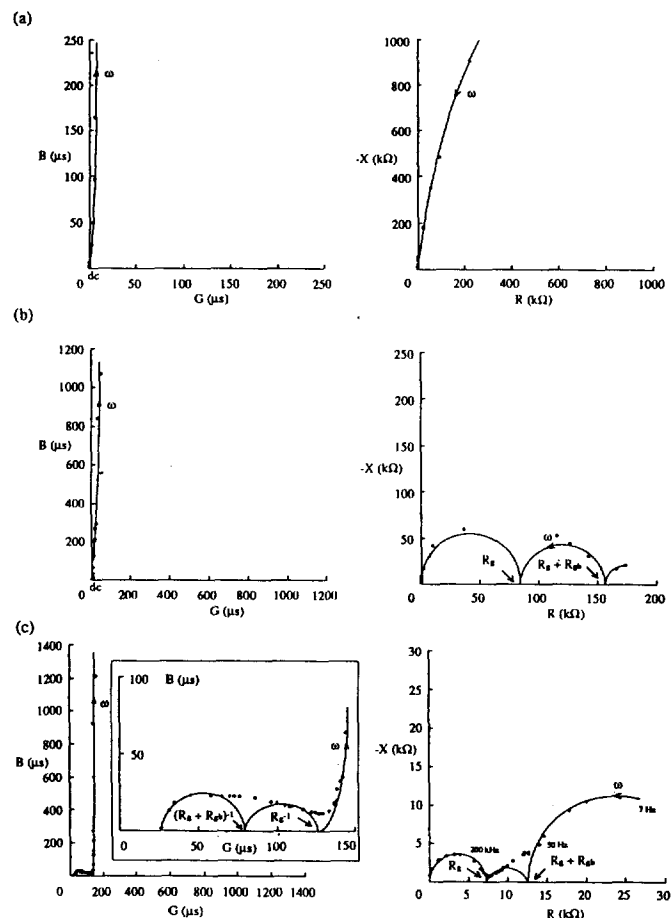


Figure 4. Plots of impedance and admittance for 25 mole % Fe-sodalite at (a) 205 °C, (b) 325 °C, and (c) 450 °C.

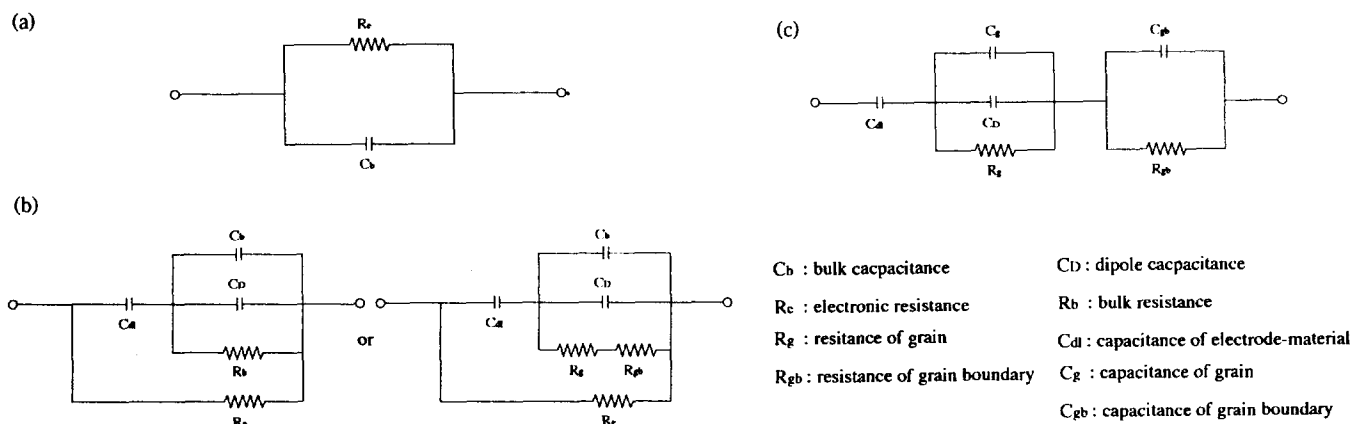
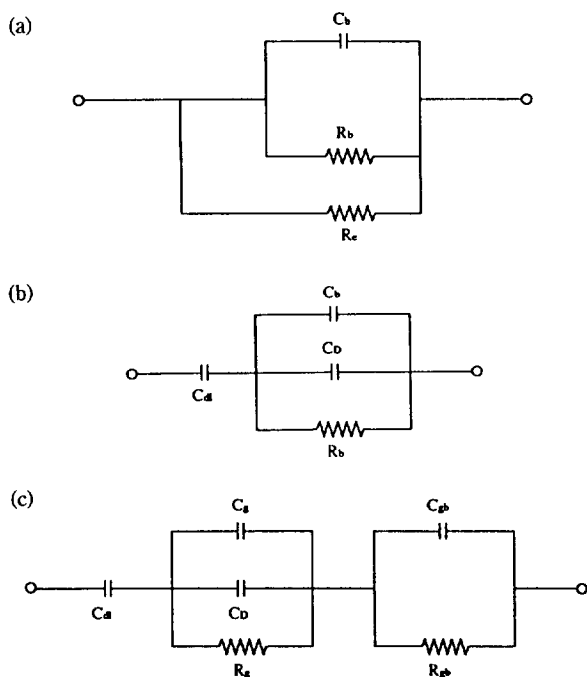


Figure 5. Equivalent circuits designed for 0, 5, 15, 20 and 25 mole % Fe-sodalite at (a) 205 °C, (b) 325 °C, and (c) 450 °C.

for the resolution of an overlapping situation.<sup>13</sup> Magnitude of electronic resistance was calculated by extrapolating the plot of  $B$  vs.  $G$  as frequency goes to zero.

At 450 °C,  $R_e$  was much lower than  $R_b$ , so the component  $R_e$  was ignored. The conductivity was mainly ionic and feasible long range migration by Na ion caused high  $C_M$  (about 100 nF) at low frequency. However,  $C_M$  also could be eliminated at high frequency resulting in  $C_b$  only. The magnitude

of  $C_b$  at 325 °C and 450 °C were 5-10 pF higher than that of 205 °C because of the dipole reorientation process, which was formed by pairing of ions. The mobile Na ions in substitutional or interstitial sites carry effective charges from anionic group, forming dipoles. The capacitance by dipole relaxation process,  $C_D$  is assumed to be arranged in parallel with  $C_b$ .<sup>6</sup> As frequency increased,  $R_g$  and  $R_{gb}$  could be estimated separately from the data of impedance and admittance. At



**Figure 6.** Equivalent circuits designed for 10 mole % Fe-sodalite at (a) 205 °C, (b) 325 °C, and (c) 450 °C.

this temperature, the plot of  $B$  vs.  $G$  showed semicircle, which meant the components  $R_b$  and  $C_d$  were arranged to series circuit at low frequency. The distorted semicircle was composed of two semicircles giving the information about  $R_g$  and  $R_{gb}$ . The equivalent circuit is drawn in Figure 5(c).

The exceptional electric character and sodium atomic percentage of 10 mole % Fe sodalite were mentioned before.  $C_d$  was not formed in the overall frequency range except  $C_b$  (40 pF) at 205 °C, and ionic migration was not active ( $10^{-6} \Omega^{-1} \text{cm}^{-1}$ ) even though 90% ionic conducting property was observed. The experimental impedance and admittance

plots in Figure 2(a) indicate parallel behavior among  $C_b$ , 90% contribution of  $R_b$  and 10%  $R_e$ . As temperature increased,  $R_e$  part was negligible and capacitance increased by the formation of  $C_d$  at low frequency. The  $C_d$  was also eliminated at above 10 kHz at 320 °C, but the trace of  $C_d$  (about 0.05% of the total  $C_d$ , but several hundreds times of  $C_b$ ) and  $C_D$  were still remained at 450 °C. Figure 6 shows the equivalent circuits of Fe 10 mole %-substituted sodalite.

**Acknowledgment.** We thank Korea Science and Engineering Foundation for financial support.

## References

1. Kim, C. H.; Jung, C. S. *Bull. Korean Chem. Soc.* **1990**, *14*, 215.
2. Bauerle, J. E. *J. Phys. Chem. Solid* **1969**, *30*, 2657.
3. Schouler, E.; Hammou, A.; Kleitz, M. *Mater. Res. Bull.* **1976**, *11*, 1137.
4. Raistrick, I. D.; Chun Ho; Huggins, R. A. *J. Electrochem. Soc.* **1976**, *123*, 1469.
5. Bayard, M. L.; Barna, G. G. *J. Electroanal. Chem.* **1978**, *91*, 201.
6. Bruce, P. G.; West, A. R. *J. Electrochem. Soc.* **1983**, *130*, 662.
7. Casciola, M.; Fabiani, D. *Solid State Ionics* **1983**, *11*, 31.
8. Subramanian, M. A.; Clearfield, A. *Mater. Res. Bull.* **1984**, *19*, 1135.
9. Kim, C. H.; Kim, E. D. *Bull. Korean Chem. Soc.* **1989**, *10*, 495.
10. Cole, K. S.; Cole, R. H. *J. Chem. Phys.* **1941**, *9*, 341.
11. Johnson, Jr., R. T.; Biefeld, R. M.; Knotek, M. L.; Morosin, B. *J. Electrochem. Soc.* **1976**, *123*, 680.
12. Wagner, C. D. ed.; *Handbook of Photoelectron Spectroscopy*; Eden Praire, **1979**.
13. Kleitz, M.; Kennedy, J. H. ed.; *Fast ion Transport in Solids*; Vashshita, Mundy and Shenoy: Elsevier North Holland Inc., 1979; p 185.